Impact of Sea-level Rise and Storm Surges on a Coastal Community

K. L. MCINNES, K. J. E. WALSH, G. D. HUBBERT and T. BEER
CSIRO, Division of Atmospheric Research, PMB 1, 3195 Aspendale, Australia
(E-mail: kathleen.mcinnes@csiro.au)

Abstract. A technique to evaluate the risk of storm tides (the combination of a storm surge and tide) under present and enhanced greenhouse conditions has been applied to Cairns on the north-eastern Australian coast. The technique combines a statistical model for cyclone occurrence with a state-of-the-art storm surge inundation model and involves the random generation of a large number of storm tide simulations. The set of simulations constitutes a synthetic record of extreme sea-level events that can be analysed to produce storm tide return periods. The use of a dynamic storm surge model with overland flooding capability means that the spatial extent of flooding is also implicitly modelled. The technique has the advantage that it can readily be modified to include projected changes to cyclone behaviour due to the enhanced greenhouse effect. Sea-level heights in the current climate for return periods of 50, 100, 500 and 1000 years have been determined to be 2.0 m, 2.3 m, 3.0 m and 3.4 m respectively. In an enhanced greenhouse climate (around 2050), projected increases in cyclone intensity and mean sea-level see these heights increase to 2.4 m, 2.8 m, 3.8 m and 4.2 m respectively. The average area inundated by events with a return period greater than 100 years is found to more than double under enhanced greenhouse conditions.

1. Introduction

Tropical cyclones pose a major threat to the northern regions of Australia due to their extreme winds, heavy rainfall and higher-than-normal sea-levels. Often, sea-level coastal flooding from the storm surge, a region of elevated sea-level generated by the strong winds and low atmospheric pressure, causes the greatest destruction from a tropical cyclone. Climate change due to the enhanced greenhouse effect has the potential to increase the risk of storm surge hazard at a given coastal location through changes to tropical cyclone characteristics and sea-level rise.

For many applications, such as the design standards for buildings and coastal infrastructure, the siting of building developments, emergency management and, indirectly, tourism, the risk of extreme events such as storm surges must be quantified. The risk is presented as a return period or an average time interval between the occurrences of two events of a particular magnitude.

The paucity of long tide gauge records, combined with the relatively rare occurrence of tropical cyclones at any given tide gauge location, means that direct analysis of observational data generally cannot be used to evaluate the risk of storm

surges. Furthermore, observational data presents information on current climate conditions and therefore cannot be used to infer the changes in risk caused by the enhanced greenhouse effect.

This study investigates the impact of climate change on extreme sea-levels due to storm tides for Cairns on the north-eastern Queensland coast. A method is used that combines a statistical model of likely cyclone behaviour with deterministic models of the coastal ocean. The range of plausible cyclone characteristics is derived from an analysis of the historical cyclone record in the region. A Monte-Carlo approach is used to randomly select cyclone characteristics from which hundreds of storm tide simulations are performed. The set of results constitutes a synthetic record of extreme sea-level events that can be analysed to produce return periods (average recurrence intervals).

The possible change to the present cyclone climatology due to the enhanced greenhouse effect is evaluated using a Regional Climate Model to simulate tropical cyclone-like lows for both the current climate and enhanced greenhouse conditions. These changes, also due to the enhanced greenhouse effect, are incorporated into the method used to generate return periods for storm tides. Finally, the impact of sea-level rise scenarios on storm tide return periods is investigated.

Previous studies along the Queensland coast have investigated storm surges and storm tides for design purposes. The most comprehensive of these was carried out by the Department of Civil and Systems Engineering at James Cook University for the Beach Protection Authority in the late 1970s, where storm surge modelling was undertaken at 10 locations along the Queensland coast (Harper *et al.*, 1977). Return periods for extreme sea-level events were subsequently evaluated for the same locations by combining the storm surge results stochastically with tides (Blain *et al.*, 1985). However, the historical cyclone data record has since been improved and technological advances in computer capability now enable considerably more complex models to be run. Storm surge modelling techniques have also been improved. These developments suggest that these original studies should be re-evaluated. The present study uses sophisticated models to evaluate storm tide return periods under present and enhanced greenhouse conditions at Cairns on the north-eastern Australian coast.

The remainder of this paper is organised as follows. The storm surge model and examples of the model simulations are presented and discussed in Section 2. The methodology for evaluating storm tide return periods and a statistical model for cyclone occurrence in the Cairns region is developed in Section 3. Section 4 presents and discusses the possible changes to cyclone behaviour and mean sea-level due to the enhanced greenhouse effect. In Section 5, return periods are determined from the storm tide simulations under present and changed climate conditions and the uncertainty and implications of the results are discussed. Finally, conclusions are presented in Section 6.
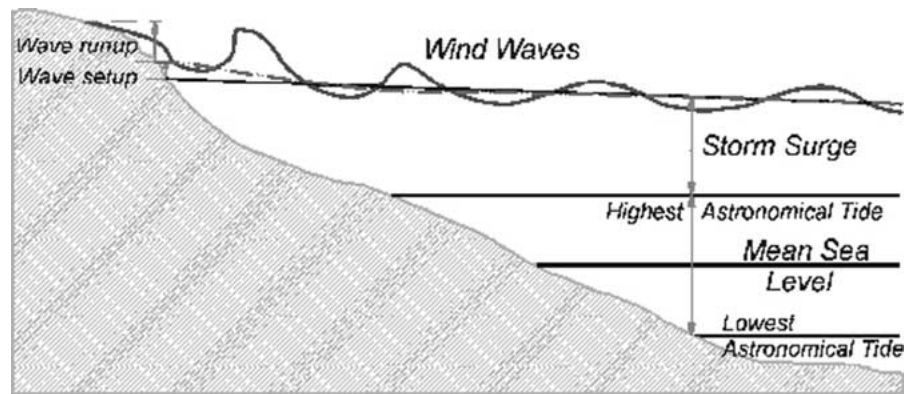
Figure 1. Contributions to extreme sea-levels at the coast.

2. Methodology

2.1. CONTRIBUTIONS TO COASTAL SEA-LEVELS

The total water level at the coast resulting from a tropical cyclone consists primarily of contributions from the storm surge and astronomical tide (see Figure 1). The storm surge is caused by the combined action of the surface wind and pressure on the ocean surface. The maximum sea-levels are generally located close to the region of maximum onshore winds as the cyclone crosses the coast. Cyclones travelling parallel to the coast will also generate elevated sea-levels if sufficiently close to the coast. It should be noted that due to the non-linear interactions of bottom friction with ocean currents, sea-level heights due to the combination of the positive tide and positive surge are generally lower than the sum of the individual components. It is for this reason that we have chosen to include tidal forcing implicitly in the model simulations in the present study, rather than adding it in later. Waves also contribute to coastal sea-levels during tropical cyclones. The net effect of breaking waves at the coast produces wave setup, and individual breaking waves produce wave run-up. Explicit calculation of these effects is neglected due to the complexity of the models required to determine their contribution; however, an allowance is made in the final results for the likely impact of wave setup.

The magnitude of the storm surge is dependent on various cyclone characteristics. The most damaging of these is wind speed that is influenced by a combination of the cyclone intensity, cyclone translational speed and the internal structure of the cyclone. A simplified representation of the wind field can be generated using the analytical cyclone model of Holland (1980), where cyclone intensity is represented by the cyclone central pressure relative to the background atmospheric pressure. The size of the cyclone is given by the distance from the cyclone centre to the region of maximum winds. Additional information required to categorise the cyclone is the translational speed of the cyclone, its direction of movement and its proximity to the region of interest.

In addition to cyclone characteristics, the depth and shape of the ocean floor can influence the storm surge height. For example, relatively wide and shallow continental shelves tend to amplify the resulting storm surge and bays flanked by headlands can further increase the elevated water levels.

2.2. STORM SURGE MODEL

The storm surge model used in this study is a depth-averaged ocean current model developed to simulate currents and sea surface elevations on continental shelves (Hubbert *et al.*, 1990, 1991; Hubbert and McInnes, 1999a,b). The model, known as GCOM2D, solves a set of fluid-dynamical equations over a grid comprised of equally spaced points in an east-west and north-south direction over the region of interest. Finer resolution grids have a greater concentration of grid points per unit area and therefore can resolve in greater detail the horizontal variation in parameters such as water depth, currents, topography and bathymetry. GCOM2D is driven by wind stresses and atmospheric pressure gradients acting on the ocean surface, sea-level heights at its lateral boundaries due to tides and atmospheric conditions, and friction of the ocean floor.

GCOM2D features a moveable coastal boundary that enables the flooding and draining (i.e. inundation) of the coastal terrain due to the storm tide to be simulated. The inundation algorithm is described in detail in Hubbert and McInnes (1999b). It is shown that sea-levels simulated at the coast are more realistic when a moveable coastal boundary is used, compared to the simpler to implement, fixed-coast storm surge models that tend to overestimate the coastal sea-levels (Yeh and Chou, 1979; Hubbert and McInnes, 1999a). Nevertheless, the accuracy of the inundation algorithm is dependent on the accuracy and resolution of the data describing the low-lying coastal terrain. In general, this algorithm is only used on grid resolutions of less than about 500 m.

An important feature of GCOM2D is that it can be run over successively finer regions utilising the results of the lower resolution, outer simulations as boundary conditions. This so-called 'nesting' technique is an economical way of maximising grid resolution over the region of interest while maintaining reasonable computational overheads.

In this study, model simulations are carried out over two regions. The lower resolution simulations are conducted with a grid spacing of 1.6 km over the entire region shown in Figure 2a. Simulations are then conducted over the smaller region centred on Cairns (Figure 2b) at 200 m resolution.

Topography of the region was obtained from the AUSLIG GEODATA 9-second Digital Elevation Model (DEM) with grid spacing of nine seconds in longitude and latitude (approximately 250 m resolution) (AUSLIG, 1994). It was enhanced in the Cairns region using data from the 50 m DEM of Zerger (1996). Bathymetry in the immediate vicinity of Cairns was obtained by manually digitising shipping charts of the region.
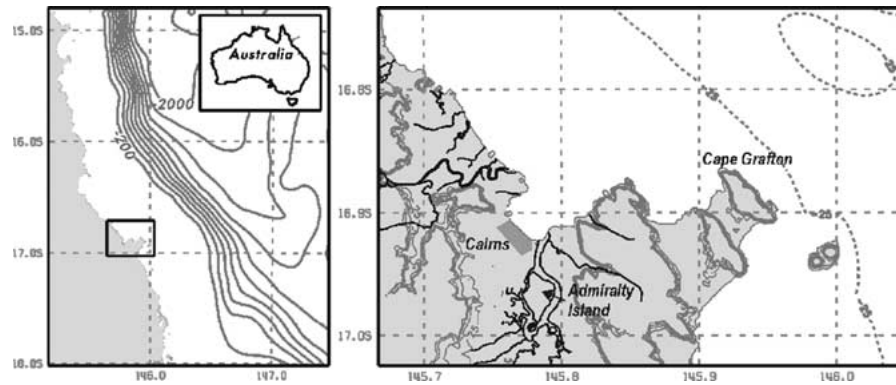
Figure 2. (a) The area covered by the low resolution storm surge model on a 1.6-km grid. Bathymetric contours are shown every 200 m. (b) The 200-m high resolution storm surge model grid. Topographic contours are shown every 25 m up to 100 m and the central business district of Cairns is indicated by darker shading.

Wind speed and pressure fields required to force the storm surge model are derived using the analytical wind profile model of Holland (1980). Cyclone profiles are determined by specifying the central pressure, radius of maximum winds, speed of forward motion, direction and the wind profile shape. The surface wind is then derived following the procedure described in Hubbert *et al.* (1991). Wave setup is not explicitly modelled in the present study. However, previous studies in northern Australia, in which wave setup was explicitly modelled, suggest that it is typically about 10% of the storm surge height (see, for example, Hubbert and McInnes, 1999a). In the present study, an allowance for wave setup is made by increasing the storm surge component of the total sea-level elevation by 10% (the storm surge component is determined by recalculating the tidal contribution at the point of interest and subtracting this value).

2.3. STORM SURGE SIMULATIONS

In this section, the nature of storm surges affecting the Cairns region is investigated using the storm surge model. In the absence of observations of severe storm tide events to use for model verification, results are compared to a previous storm surge modelling study conducted in the Cairns region. The model is also used to illustrate the effect on the storm surge of different directions of approach of the cyclone.

A set of storm surge simulations is carried out on the low resolution grid forced by four coastal crossing cyclones with central pressures and forward speeds of 945 hPa and 28 km hr^{-1} respectively, as well as one coast-parallel cyclone. The directions of approach of the coastal crossing cyclones are 355°, 35°, 75° and 105° respectively. Here, direction is defined as the bearing from which the cyclone approaches i.e. a bearing of 0° means a cyclone approaching from the north. Each cyclone is configured to make landfall just to the north of Cairns so as to place the
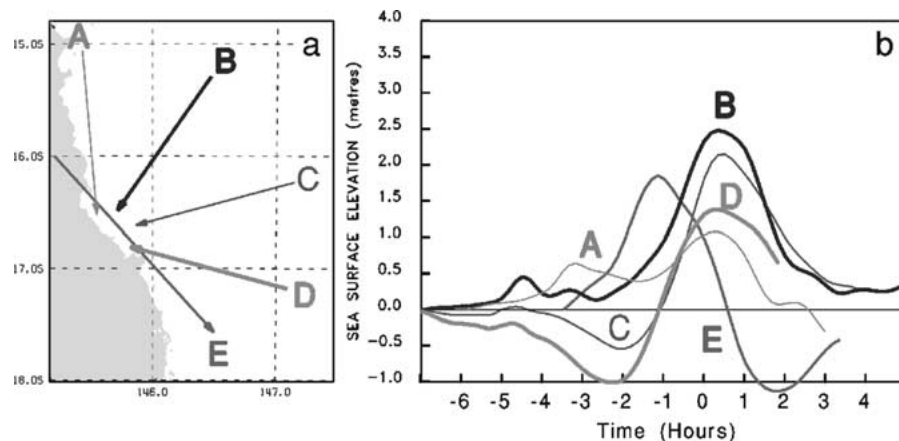
Figure 3. (a) Cyclone tracks for cyclones of central pressure 945 hPa and forward speed of 28 km hr^{-1}, and (b) the resulting simulated sea-level heights. Times shown are relative to the time of coastal crossing.

most intense onshore winds in the vicinity of Cairns. Tidal oscillations are ignored to simplify the interpretation of the results, and sea-level heights are expressed relative to the Australian Height Datum (AHD, approximately mean sea-level).

The cyclone paths are shown in Figure 3a, while time series of the sea-level heights at Cairns are shown in Figure 3b. Cyclones A and B produce onshore winds at all times during the approach of the cyclone and therefore produce positive sea-levels in the lead up to the peak. The most pronounced surge is produced by cyclone B, which peaks at 2.5 m. The cyclone winds at the time of landfall are shown for this case in Figure 4a, while the resulting storm surge is shown in Figure 4b. Elevated sea-levels affect about 150 km of coastline. The headland situated to the east of Cairns assists in focussing the most severe part of the storm surge at Cairns for cyclones approaching from this general direction.

Cyclones C and D produce weak negative sea surface elevations in the first half of the simulation, due to the predominantly offshore winds at the coast as the cyclone approaches. The surge peaks are also of lower magnitude and shorter duration. Cyclone D produces a lower surge of 1.3 m due to the protection from the wind and surge offered to Cairns by Cape Grafton to the east. Cyclone E produces a positive surge until the cyclone centre passes to the south of Cairns, after which time offshore winds generate a negative surge.

Cyclones A, B and C can be compared with similar results produced by Harper *et al.* (1977). In the present study, these cyclones produced peak storm surges of 1.0, 2.5 and 2.2 m respectively, whereas, in Harper *et al.*, the equivalent surge heights were 0.8, 2.2 and 2.0 m respectively. The differences between the maximum heights in the two studies are likely to be due to the differences in model resolution (1.6 km in the present study and 9.3 km in the Harper *et al.* study).
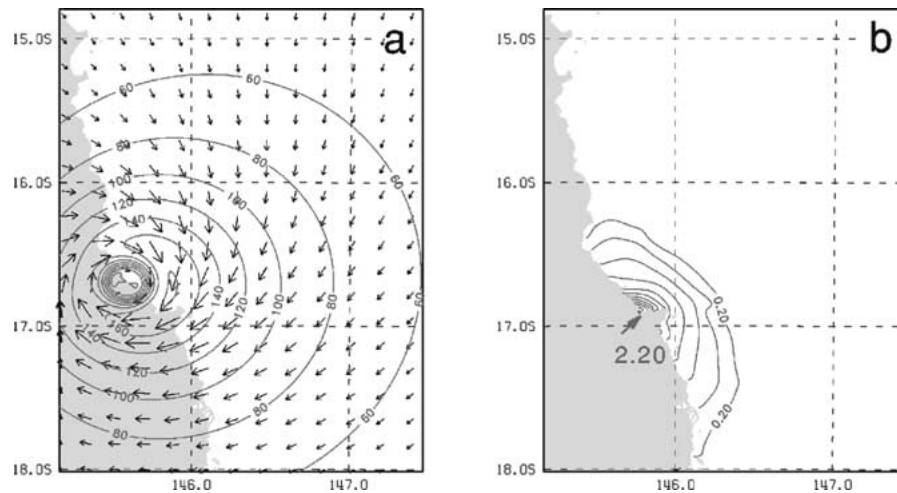
Figure 4. (a) Wind vectors and contours of wind speed for cyclone B as it crosses the coast, and in (b) the sea-level elevations at the time of coastal crossing. Contours of wind speed are shown every 20 km hr^{-1} and sea-level contours are shown every 0.2 m. Sea-level heights are relative to AHD.

These results illustrate the variation in storm surge strength and duration that occurs under different directions of cyclone approach. The most intense storm surges can be expected to occur for cyclones approaching from the northeast, assuming all other factors are constant.

3. Methodology for Storm Tide Return Periods

3.1. OVERVIEW

The return period is the average amount of time between the occurrence of events of a particular magnitude. In mathematical terms, it is the inverse of the probability of the event occurring. A key requirement of the methodology employed in the present study is that the cyclone characteristics that influence storm surge height can be represented in probabilistic terms. In this way many randomly selected cyclones yield a plausible population of events that may be expected to influence a location over a long time interval. The major factors contributing to the evaluation of the storm tide return periods are illustrated in Figure 5. The various cyclone characteristics influence the storm surge height while the date and time of the cyclone determine the phasing of the tide and surge.

An estimate of the average frequency of tropical cyclone occurrence is important in converting the hundreds of random storm tide simulations into an effective time series from which the return periods can be calculated. For example, if, on average, a cyclone affects a coastal location once every five years, then each randomly performed simulation represents five years of data. The maximum storm
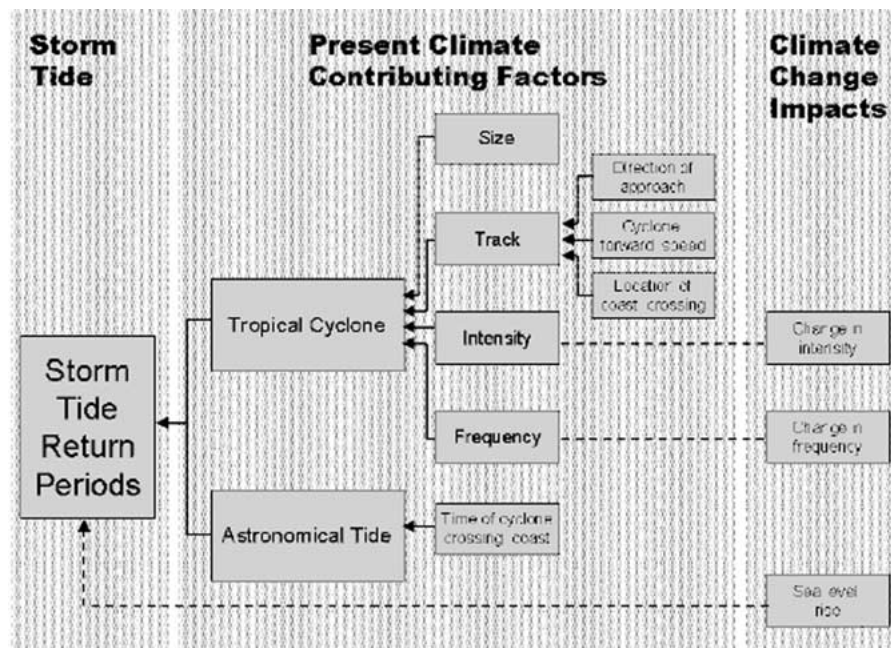
Figure 5. Schematic diagram illustrating the key factors considered in the present study that are likely to affect storm tide return periods under present and enhanced greenhouse climate conditions.

tides resulting from all simulations performed can then be sorted and ranked against their expected recurrence interval.

Since not all cyclones impacting on a region actually make landfall, coast-parallel cyclone tracks should also be considered, even though these will, in general, only contribute to the low amplitude end of the statistics. Simulations are therefore conducted for cyclones with a coast-parallel direction of movement. All other characteristics are randomly selected. A number of coast-parallel cyclone simulations is combined with the coastal crossing cyclone simulations, based on the observed ratio of each type recorded in the historical record.

The evaluation of return periods under enhanced greenhouse conditions involves modifying the statistical model of present day cyclone occurrence, consistent with the latest understanding of changes to tropical cyclone behaviour, then repeating the random storm tide simulations. The most important impacts likely under enhanced greenhouse conditions are shown in Figure 5. The modifications to the tropical cyclone characteristics are discussed in Section 4. The impact of a mean sea-level rise on the results is also investigated.
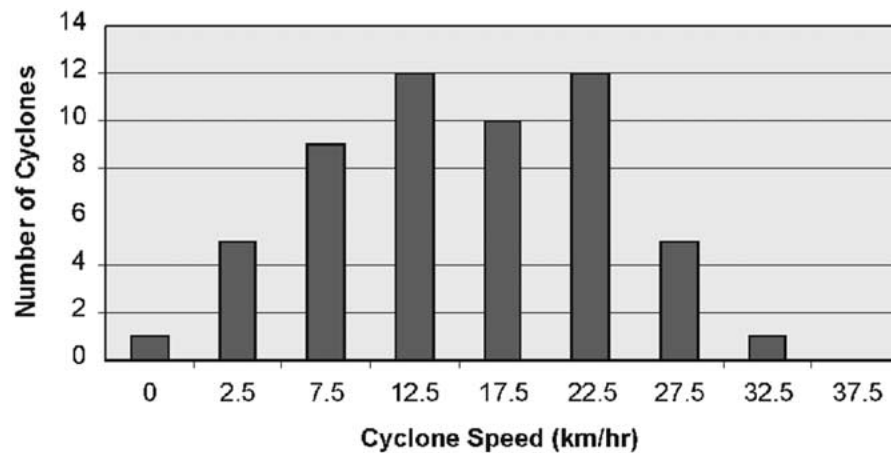
Figure 6. Frequency distribution for cyclone forward speeds for coastal crossing cyclones occurring between 14° S and 20° S.

3.2. CYCLONE CLIMATOLOGY

In this section, a statistical model of cyclone behaviour is developed from an analysis of historical events that have occurred in the Cairns region. Cyclones occurring in the Australian region from 1907 to 1997 have been documented by the Bureau of Meteorology and were used to determine the characteristics and frequency of cyclones affecting Cairns. Since few cyclones have occurred in the immediate vicinity of Cairns in this time, a broader coastal region was considered to be representative of the Cairns area. The construction of the probability distribution functions for the various cyclone characteristics are now examined in turn.

Track

The cyclone track is characterized by the forward speed, direction of approach and location of coastal crossing of the tropical cyclone. Cyclones crossing the coast between 14° S–20° S were used to establish probability distribution parameters. This covers about 375 km of coastline with Cairns at its centre. A total of 55 cyclones were counted in this region.

Cyclone forward speeds, binned into 5 km hr^{-1} classes (Figure 6), and direction data organized into 15° bins (Figure 7) were found to satisfy the chi-squared test of normality at the 95% confidence level and were therefore approximated using a normal distribution. The distribution for cyclone speed was characterised by a mean and standard deviation of 15.5 km hr^{-1} and 6.6 km hr^{-1} respectively while the direction data was approximated with a mean and standard deviation of 63.8° and 27.1° respectively.

Location of coastal crossing strongly influences the peak storm surge at the point of interest. For example, simulations presented in Section 3 indicate that
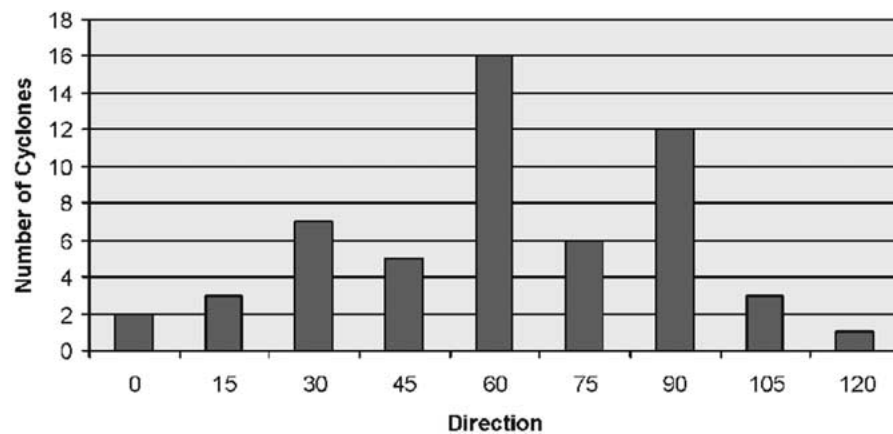
Figure 7. Frequency distribution for cyclone directions at the time of coastal crossing for cyclones occurring between 14° S and 20° S. Directions are in degrees clockwise from north.

cyclones crossing the coast at Cairns or up to about 100 km to the north are likely to produce a storm surge effect at Cairns. Cyclones crossing to the south of this region produce offshore winds and hence negative sea surface elevations at Cairns. In the random simulations, the location where the tropical cyclone makes landfall is randomly chosen and evenly distributed along the coast between 16° S and 17° S. Clearly, the most severe storm surges will occur for cyclones crossing the coast closer to Cairns.

As shown in Figure 3b, cyclones that travel parallel to the coast can also cause storm surges, although these surges will mainly contribute to the low amplitude end of the statistics. In the present study, storm tide simulations are conducted for coast-parallel cyclones. The same probability distribution functions that are developed for coastal crossing cyclones are used for the coast-parallel cyclones except for direction, which is kept constant at 335°, and distance from coast, which can vary from 0 to 100 km from the coast with equal likelihood. Beyond 100 km, model simulations based on a cyclone with the characteristics used in Section 2.3 did not produce a storm surge at Cairns. The ratio of coastal crossing to coast-parallel cyclones is taken to be 85:15 based on the numbers of each category occurring historically in the search region.

Size

The size of the tropical cyclone, generally measured as the radius from the centre to the region of maximum winds, could not be categorized statistically due to an absence of data. As a consequence and, following common practice, a fixed value of 30 km was assigned to this parameter in all randomly selected cyclones.

Cyclone Intensity

Probabilities for cyclone intensity were estimated using extreme value theory. All central pressures of cyclones that crossed the coast between 14° S and 20° S or passed within 1° of the coast within this latitude range in the 90 years since the beginning of the record in 1907 were considered. The central pressure at the time of crossing the coast or when the cyclone was at the closest point to the coast was used. The reason for this is that cyclones tend to fill once they cross the coast and so to use a deeper central pressure if the cyclone was further offshore may have biased the distribution towards more extreme cyclones. In addition to this, the modelling procedure is based on only coast crossing cyclones or cyclones that follow a coast-parallel path within 1° of the coast and so cyclones that occurred further offshore were not considered.

The lowest biennial central pressures were extracted from the data with a value of 1,000 hPa being used for pairs of years where no cyclone occurred. Following common practice, the Type I Extreme Value Distribution or Gumbel distribution was fitted to the data, where the probability that the central pressure P is less than some pressure P_o is given by

$$\Pr(P < P_o) = e^{-e^{\frac{-(P_o-a)}{b}}} \tag{1}$$

where $a = \bar{P} - \gamma b$ and $b = \sigma\sqrt{6}/\pi$ are the location and scale parameters respectively, with σ being the standard deviation, $\bar{P}$ the mean pressure of the distribution and $\gamma = 0.57721$ is Euler's constant. Using the method of moments, the moment estimators were found to be $a = 996.4$ and $b = 11.2$ respectively. Based on these values, the return period curve for central pressure is shown in Figure 8 along with the 95% data confidence limits. Selected cyclone return periods are given in Table I. The exceedence probabilities were then converted to probabilities of occurrence for intensities within designated pressure ranges.

We note that prior to the 1960's when satellite observations became available, cyclone data is generally less reliable (Holland, 1981). However, since the fitting of a Gumbel distribution requires knowledge of only the deepest cyclone to have occurred in a designated time interval (biennially as is used in the present study), it was felt that the particularly severe coast-crossing cyclones were less likely to go unobserved in the earlier period.

Cyclone Frequency

The average annual frequency of cyclones affecting Cairns enables a time scale to be assigned to the model generated storm tide results. Lourenz (1981) analysed cyclones in the Australian region over the 70 years up to 1980. Based on this study, 11 cyclones have crossed the coast over the stretch of coastline 100 km to the north of Cairns, yielding a frequency of about one cyclone every six years. The frequency has not changed appreciably if one also includes cyclones that have occurred since
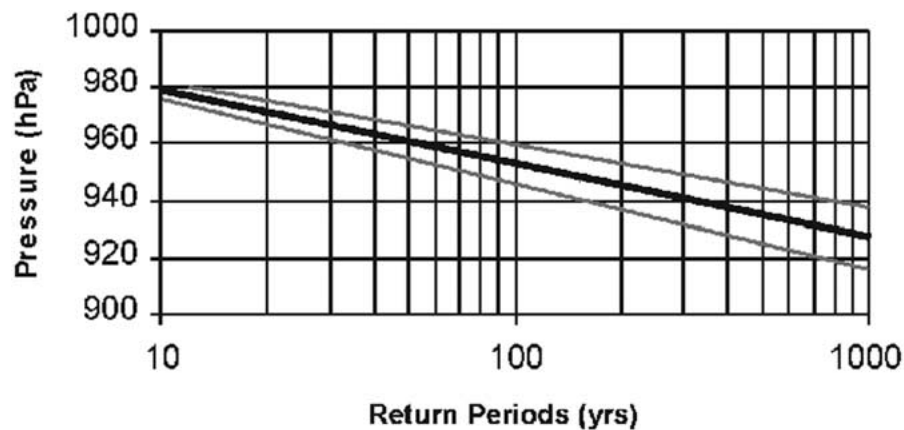
Figure 8. Central pressure return period curves for Cairns with 95% confidence limits.

Table I. Return periods (yrs) for given cyclone intensities (hPa) under present and enhanced greenhouse climate conditions based on cyclones crossing the coast or passing within 1° of the coast between latitudes 14° S and 20° S

Return Period (years)	Central Pressure (hPa) for present climate	Central Pressure (hPa) for enhanced greenhouse climate
10	979	966
20	971	956
50	963	941
100	953	931
200	945	920
500	935	907
1000	927	887

that time. If one also includes coast-parallel cyclones within the distance from the coast that is considered in the present study, this alters the frequency of cyclones to approximately one every five years.

Tides

The inclusion of tides in storm surge calculations is important because of the non-linear way in which tides and surges interact. The relative phasing of the tide with the storm surge is achieved by randomly selecting a time associated with the cyclone occurrence. The tides themselves vary in amplitude throughout the year. Cairns, which experiences a predominantly diurnal tidal regime, has a highest astronomical tide (HAT) of 1.8 m above AHD (HAT occurs once every 18.6 years).
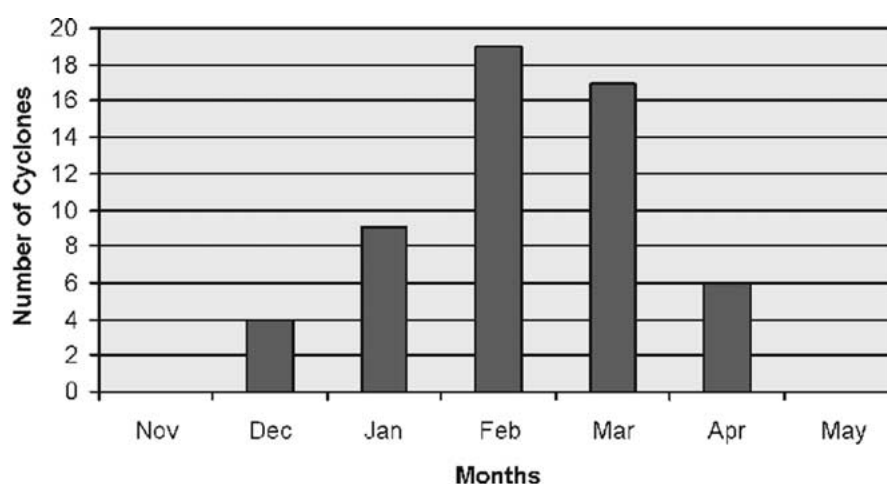
Figure 9. Frequency distribution for monthly cyclone occurrence in the Cairns region.

The mean highest high water (MHHW), or in other words the average value of the highest high tide of the day, is about 1 m above AHD. To take into account tidal variations throughout the year, monthly cyclone occurrence in the region was also analysed (Figure 9). This was also approximated using a normal distribution.

3.3. CYCLONE SELECTION

Once cyclone behaviour in the Cairns region has been analysed, cyclones can be constructed by randomly selecting the various cyclone characteristics. The use of the probability distribution functions defined in the previous section ensure that the least common characteristics, such as extremely intense cyclones, are selected only very rarely while weaker cyclones are more frequently selected.

4. The Impact of Climate Change

In a warming climate, two factors may act to increase the risk of storm tides. These are possible changes in cyclone characteristics, such as intensities and frequencies, and mean sea-level rise.

4.1. CYCLONE INTENSITY

Latest scientific estimates suggest that modest to moderate (0-20%) increases in average and maximum cyclone intensities are expected in the Australian region in a warmer world. For $2 \times CO_2$ conditions (about 2050), we have assumed an increase in mean cyclone intensity based on the results of Walsh and Ryan (2000). In that study, a large number of Tropical Cyclone-Like Vortices (TCLVs) in both

the present and enhanced climate simulations of a regional climate model were selected for re-simulation at a higher model resolution. Cyclones of central pressure 985 hPa were then inserted at the position of the original TCLV and a higher-resolution simulation conducted to allow the cyclone to develop to its maximum intensity. Comparing the maximum intensities of the cyclones in the two climates indicated that under enhanced greenhouse conditions, the average intensity of cyclones was 10 hPa deeper and the standard deviation had increased by 5 hPa. We note, however, that these changes represent an upper threshold for changed climate conditions because, in Walsh and Ryan (2000) the changed means and standard deviations were derived after inserting relatively intense (985 hPa) cyclones into the higher-resolution simulation. For less intense cyclones, it is possible that the average increase in intensity in changed climate conditions may be somewhat less than this.

These figures are consistent with theoretical techniques that estimate changes in maximum potential intensity (MPI) of tropical cyclones for the Australian region (e.g. Holland, 1997). These theoretical techniques also suggest increases in maximum tropical cyclone intensities in the Australian region of similar magnitude, when the tail of the fitted distribution is examined. Nevertheless, these estimates remain uncertain and may be refined further in the future as better simulations become available.

The mean and standard deviation of the observed cyclone data set are modified with the changed values for the enhanced climate simulation. This yields changes to the moment estimators of the Gumbel distribution so that $a = 988.5$ and $b = 14.8$. The probabilities resulting from the modified distribution are evaluated and used as a basis for the randomly selected cyclone intensities for the enhanced climate storm tide simulations (see Table I).

4.2. CYCLONE FREQUENCY

Changes in the numbers of cyclones in the Australian region caused by the enhanced greenhouse effect remain unknown, as cyclone numbers are strongly associated with the ENSO phenomenon, the exact nature of which in a warmer world is currently unknown. Too little is also known about the effect of climate change on the mid-level winds that govern typical tropical cyclone directions of movement. Therefore, in this study, we assume no change to cyclone frequency or cyclone directions in the enhanced greenhouse climate scenario.

4.3. SEA-LEVEL RISE

Sea-level rise as a consequence of the enhanced greenhouse effect is one of the more confident results of climate change research (IPCC, 1996, 2001). Global sea-level rise over the next few decades is expected from several sources. These include thermal expansion of the oceans, melting of glaciers and small ice sheets, and

Table II. Low, mid and high estimates of global mean sea-level rise (in cm) for the years 2020 and 2050 (IPCC, 1996), relative to 1990

Year	Low	Mid	High
2020	5	10	20
2050	10	20	40

changes in the accumulation of snow and ice in Antarctica and Greenland. Estimates of changes to these components are made using predictions of future warming from climate models. These models are complex numerical representations of the Earth's ocean and atmosphere and, depending on how the physical processes in the models are represented, they predict a range of different warmings for a specified increase in greenhouse gases. Furthermore, there is considerable uncertainty regarding the future emissions of greenhouse gases and associated aerosols, as the amount of these emissions depends upon the character and scale of future economic activity, which is difficult to predict. Therefore, predictions of mean global sea-level rise are usually given as a range encompassing several different scenarios (Table II), depending upon the amount of future emissions assumed. In the present study, we use the mid-range estimate of sea-level rise for 2050 of 20 cm.

5. Return Period Estimates

5.1. CONTROL CLIMATE

The maximum sea-level heights from each of the 1000 simulations are sorted and ranked against their expected recurrence interval (e.g. assuming one cyclone every 5 years, the highest event is the 1-in- 5000 year event and the fifth highest is the 1-in-1000 year event). The line of best fit is estimated using the method of least squares and is shown in Figure 10 (note that the values include an allowance for wave setup). In addition to the current and enhanced climate simulations, upper and lower bounds on each curve have also been estimated for the 95% confidence limits of cyclone central pressure. These estimates are achieved by pooling all simulations and selecting a modified set of runs that satisfies the probability distribution curves defining the confidence limits. These confidence limits are also shown in Figure 10.

The results suggest that a storm tide will exceed HAT on average only once every 40 years or more. This result is not surprising considering the relatively low frequency of cyclones in Cairns as well as the many other factors that must combine adversely to produce storm tides that are higher than this value. Nevertheless, we
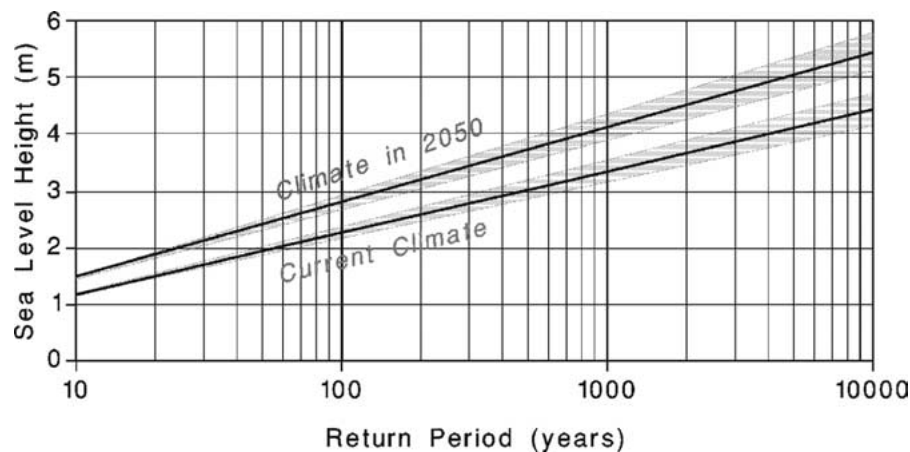
Figure 10. Return periods for storm tides at Cairns under present and enhanced greenhouse climate conditions. Error bars pertain to the 95% confidence limits on the cyclone intensity. The enhanced greenhouse climate curves relate to changes in cyclone intensity and not changes in mean sea-level.

note that the results from the present study are up to 10% lower than previous storm tide studies conducted in this region (Harper, 1999).

We now examine the extent of inland flooding implied by the results presented above. In each model simulation, the maximum sea-level attained at each model grid point due to overland flooding is stored for later analysis. The average extent of inland flooding calculated from the highest 5% of storm tide simulations is shown in Figure 11a. The results correspond with events with a 100-year or greater return period. This figure indicates that much of the township of Cairns remains above the flood line and most of the inundation is confined to the wetlands in the vicinity of Admiralty Island to the southeast of the township (Figure 2b). The inundated area represented in this diagram is approximately 32 km^2 although, we note that due to the relatively low horizontal resolution of the fine mesh model grid (200 m) in this study, these results should be seen as only broadly indicative of the areas most vulnerable to flooding due to extreme sea-level events. These figures do not include an allowance for wave setup. Finally, it must be stressed that the degree of inundation caused by a storm surge of a particular level at the coast can vary depending on the cyclone characteristics such as wind direction, duration of storm and so on. For example, greater inland penetration of floodwaters may occur for a storm of longer duration, all other things being equal.

5.2. ENHANCED CLIMATE

Storm tide heights for given return periods under enhanced climate conditions are shown in Figure 10 and selected values are also presented in Table III. These results are based on the possible increases in cyclone intensity due to the enhanced
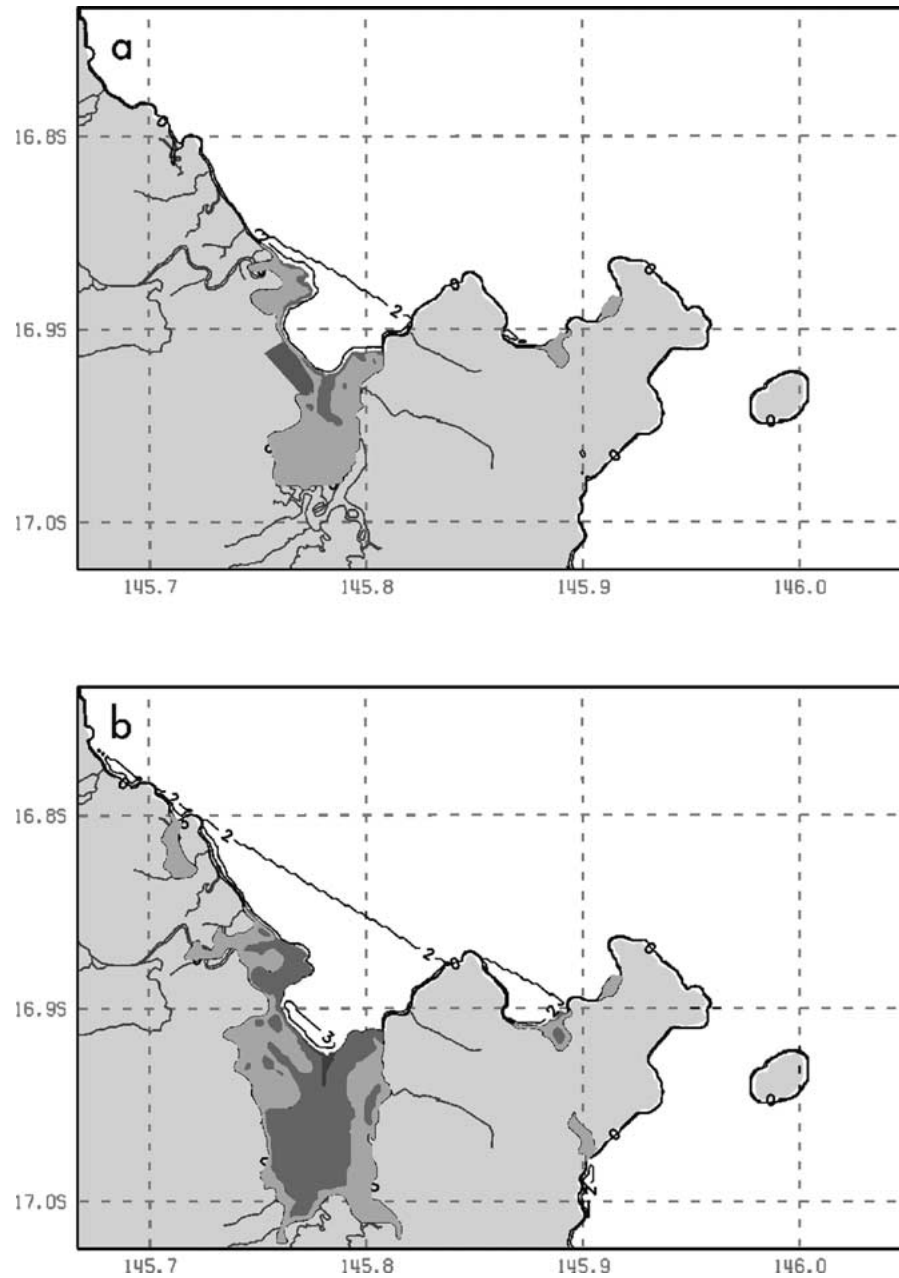
Figure 11. The average area of flooding produced by the top 5% of modelled storm surges (corresponding to a return period of 100 years or greater) in (a) the control climate and (b) the enhanced greenhouse climate. Flood levels (bold lines) are in 1 m contour intervals and are relative to the land surface over land and mean sea-level over water.

Table III. Return periods for sea-level heights under present and enhanced greenhouse climate conditions (about 2050). The fourth column includes a 20-cm sea-level rise, with error bars calculated by adding the upper or subtracting the lower sea-level rise estimates shown in Table III

Return period (years)	Sea-level height (metres)		
	Control climate	Enhanced greenhouse climate (cyclone intensity changes only)	Enhanced greenhouse climate (cyclone intensity and sea-level rise)
1000	3.4 ± 0.2	3.9 ± 0.3	4.1 (+0.5/−0.4)
500	3.0 ± 0.2	3.5 ± 0.2	3.7 (+0.4/−0.3)
200	2.6 ± 0.2	3.0 ± 0.2	3.2 (+0.4/−0.3)
100	2.3 ± 0.1	2.6 ± 0.1	2.8 (+0.3/−0.2)
50	2.0 ± 0.1	2.2 ± 0.1	2.4 (+0.3/−0.2)

greenhouse effect and result in 100-year sea-levels that are about 0.3 m higher than under control climate conditions. Alternatively, a 100-year event under current climate conditions becomes approximately a 55-year event when increases in cyclone intensity are included.

The average extent of overland flooding caused by the highest 5% of simulated storm surges under enhanced greenhouse conditions is shown in Figure 11b. Again, it should be noted that there is no wave setup or sea-level rise included in the overland flooding extent and due to model resolution, the results should only be seen as broadly indicative of the areas most at risk. Clearly, there is a much greater impact of severe sea-level events when changes in cyclone intensities are taken into account. The areal extent of overland flooding has more than doubled to approximately 71 km^2 and encompasses much of the Cairns downtown region. These results suggest that changes to cyclone intensity under enhanced greenhouse conditions would cause a considerable increase in the risk to existing infrastructure and the tourism industry of the Cairns region.

Enhanced greenhouse climate storm tide heights that include sea-level rise are also shown in Table III and indicate an even greater risk of severe storm tide. The 100-year event under current climate conditions becomes approximately a 40-year event when a sea-level rise of 20 cm is added to the enhanced climate return periods. The final column of Table III includes the mid-range estimate of sea- level rise by 2050 of 20 cm. However, it should be noted that sea-level rise at this time could be as high as 40 cm.

5.3. DISCUSSION

The 1-in-100 year return period of sea-level heights is commonly used for planning purposes. In this study, the 1-in-100 year event in 2050 is predicted to increase by about 0.5 m. As to whether this would represent an increase sufficient to require consideration in planning or disaster management is a matter for the responsible authorities. A few general comments can be made regarding the use of these results, however. It would be unwise to rely on the central estimates of return period increase for planning purposes. This is because planning requires that conservative assumptions are made, and the central estimate of return period increase would, by definition, have about a 50% chance of occurrence. An example of this issue is provided by recommendations made to the Gold Coast City Council regarding the amount of mean sea-level rise to be assumed for planning purposes (Betts, 1999). Although the central estimate of mean sea-level rise by the year 2050 is about 20 cm, Betts (1999) suggests a value of 30 cm would be more conservative and therefore more appropriate for planning purposes. Similar assumptions would need to be made about the results presented here.

A number of other uncertainties arise from the modelling methodology used in this report. These include the quality of the climate model's simulations of tropical cyclone intensity, and the shortness of the observed cyclone record used to establish the distributions of observed cyclone characteristics. In addition, climate models project a substantial range of future climates, and the projections here only represent a plausible estimate of future impact.

The statistical distributions fitted to the available data also present a source of uncertainty in the results. An example is the choice of the Type I Extreme Value Distribution or Gumbel distribution for the cyclone intensity. One particular drawback, as noted by Holmes and Moriarty (1999), is that the values predicted by the distribution are unbounded as the return period increases. This property is not strictly compatible with cyclone intensity that is constrained by maximum potential intensity considerations. Holmes and Moriarty point out that the Generalized Pareto Distribution (GPD) has similar properties to the Type III Extreme Value Distribution (or Weibull distribution), and tends to a limiting value at high return periods and is therefore more suitable for geophysical applications. Another advantage of the GPD is that it makes use of all available data rather than just the annual (or in this case, the biennial) maximum. Though in the present study, the Gumbel distribution was chosen due to its relatively widespread application in similar studies (e.g. Harper *et al.*, 1977), in future studies it is planned to examine the suitability of alternative distributions for cyclone intensity in greater detail.

6. Conclusions

Severe storm surges caused by tropical cyclones are comparatively rare events, especially when considered at a single location. As a consequence, sophisticated methods are required to evaluate their risk. The present study has combined a stat-

istical model for cyclone occurrence with a state-of-the-art storm surge inundation model to generate a synthetic record of extreme sea-level events from which storm tide return periods can be evaluated. The technique has the advantage that projected changes to cyclone behaviour caused by the enhanced greenhouse effect can be easily incorporated. While the focus of the present study has been on one location in tropical north-eastern Australia, the methodology is widely applicable to any location where extreme meteorological events can be categorised on the basis of historical behaviour.

We note that the conclusions of this study are affected by a number of sources of uncertainty that are independent of the quality of the models used here. These include the quality of historical meteorological data on extreme events and the choice of statistical functions chosen to represent their occurrence. As well as this is the accuracy of data required by the storm surge model such as bathymetry and topography, and the model resolution. An additional source of uncertainty that may influence the results of the present study is the impact of ENSO on tropical cyclone numbers in the Australian region. The state of ENSO in a warmer world is currently unknown, although a number of recent results are suggesting a trend towards a more *El Niño*-like mean state (see for instance Walsh *et al.*, 1999 for a summary of this issue). All other things being equal, this should lead to fewer cyclones crossing the Queensland coast (e.g. Basher and Zheng, 1995). Because of the generally inadequate simulation of ENSO in climate models, it is difficult to quantify this uncertainty properly. An estimate of the influence that changes in ENSO may have on tropical cyclone numbers can be obtained by comparing the 1-in-100 year return periods in the current and enhanced greenhouse climates in Table III. The 1-in-100 year sea-level height for the current climate is estimated to be 2.3 m, while in the enhanced greenhouse climate it is 2.8 m. In the current climate, a sea-level of 2.8 m corresponds roughly to a 1- in-300 year return period. Therefore, to completely negate the effect of increased cyclone intensity and sea-level rise, the number of intense cyclones in the enhanced greenhouse climate would have to fall by about a factor of three. This is a very large change compared to the current year-to-year variability in cyclone numbers, and as a result, it is unlikely. Therefore, changes in ENSO are unlikely to completely negate the anticipated increase in the 1-in-100 year return period sea-level. It should also be noted that a reduction in cyclone frequency due to such changes in ENSO is not likely in regions where cyclone numbers are less influenced by ENSO or where they experience the opposite conditions during *El Niño* events.

The methodology has been applied to Cairns on the north-eastern Australian coast. Sea-level heights in the current climate for return periods of 50, 100, 500 and 1000 years have been determined to be 2.0 m, 2.3 m, 3.0 m and 3.4 m respectively. In an enhanced greenhouse climate (around 2050), these increase to 2.4 m, 2.8 m, 3.8 m and 4.2 m respectively. The average area inundated by events with a return period of 100 years is found to more than double that under present climate conditions.

References

AUSLIG: 1994, GEODATA TOPO-250K Data User Guide, Version 1 Data, Ed 2. Australian Survey-ing & Land Information Group, Commonwealth Department of Industry, Science and Resources, Canberra, Australia.

Basher, R.E. and Zheng, X.: 1995, Tropical cyclones in the southwest Pacific: spatial patterns and relationships to Southern Oscillation and sea surface temperature, *J. Climate* **8**, 1249–1260.

Betts, H.: 1999, The implication of future climate change on floodplain planning at Gold Coast City. Proceedings, NSW Floodplain Managers' Conference, May 1999.

Blain, Bremner & Williams Pty. Ltd.: 1985, Storm tide statistics – methodology. Prepared for the Beach Protection Authority, Dept. of Environment, Queensland. 25 pp.

Harper, B.: 1999, Storm tide threat in Queensland: history, prediction and relative risks, Queensland Department of Environment and Heritage, Conservation technical report No. 10. 24 pp.

Harper, B. A., Sobey, R. J., and Stark, K. P.: 1977, Numerical simulation of tropical cyclone storm surge along the Queensland coast, Part III – Cairns. Department of Civil and Systems Engineering, James Cook University, Townsville. 15 pp.

Holland, G. J.: 1980, An analytical model of the wind and pressure profiles in hurricanes, *Mon. Wea. Rev.* **108**, 1212–1218.

Holland, G. J.: 1981, On the quality of the Australian tropical cyclone data base, *Aust. Met. Mag.* **29**, 169–181.

Holland, G. J.: 1997, The maximum potential intensity of tropical cyclones, *J. Atmos. Sci.* **54**, 2519–2541.

Holmes, J. D. and Moriarty, W. W.: 1999, Application of the Generalised Pareto Distribution to wind engineering, *J. Wind Engineering and Industrial Aerodynamics* **83**, 1– 10.

Hubbert, G. D., Holland, G. J., Leslie, L. M., and Manton, M. J.: 1991, A real-time system for forecasting tropical cyclone storm surges, *Weather and Forecasting* **6**, 86–97.

Hubbert, G. D., Leslie, L. M., and Manton, M. J.: 1990, A storm surge model for the Australian region, *Quart. J. Roy. Met. Soc.* **116**, 1005–1020.

Hubbert, G. D. and McInnes, K. L.: 1999a, A storm surge inundation model for coastal planning and impact studies, *J. Coastal Research* **15**, 168–185.

Hubbert, G. D. and McInnes, K. L.: 1999b, Modelling storm surges and coastal ocean flooding, In: B. J. Noye (ed.), *Modelling coastal sea processes*, World Scientific Publishing Co., pp. 159–187.

IPCC: 1996, *Climate change 1995: the science of climate change*, Contribution of Working Group I to the second assessment report of the intergovernmental panel on climate change, Cambridge University Press, 572 pp.

IPCC: 2001, *Climate change 2001 – the scientific basis*, Cambridge University Press, 881 pp.

Lourenz, A.: 1981, Tropical cyclones in the Australian region: July 1909 to June 1980, Bureau of Meteorology report, October 1981.

Walsh, K., Allan, R., Jones, R., Pittock, A. B., Suppiah, R., and Whetton, P.: 1999, *Climate change in Queensland under enhanced greenhouse conditions*, CSIRO Atmospheric Research, PMB 1, Aspendale, VIC. 3195, Australia. 84 pp.

Walsh, K. J. E. and Ryan, B. F.: 2000, Tropical cyclone intensity increase near Australia as a result of climate change, *J. Climate* **13**, 3029–3036.

Yeh, G.-T. and Chou, F.-K.: 1979, Moving boundary numerical surge model, *J. Waterw. Port Coastal and Ocean Div.* **105**, 247–263.

Zerger, A.: 1996, Application of spatial analysis and GIS for modelling risk in storm surge prone areas of northern Queensland, *Proc. National Disaster Reduction Conference*, Surfers Paradise, Queensland, Sept. 1996, Inst. Eng. Australia, pp. 99–106.